February 8th 2019

Supplementary Information

Formation of an Interlocked Double-Chain from an Organic-Inorganic [2]Rotaxane

Jesús Ferrando-Soria,[a,b] Antonio Fernandez,[a,c] Iñigo J. Vitorica-Yrezabal,[a] Deepak Asthana,[a] Christopher A. Muryn,[a] Floriana Tuna,[a] Grigore A. Timco[a] and Richard E. P. Winpenny[a]*

[a]*School of Chemistry and Photon Science Institute, The University of Manchester, Oxford Road, Manchester M13 9PL, UK.*
[b]*Departamento de Química Inorgánica, Instituto de Ciencia Molecular (ICMol), Universidad de Valencia, 46980 Paterna, Valencia, Spain.*
[c] *Chemistry Department, Sir David Davies Building, Loughborough University, LE11 3TU, UK.*

Table of Contents:

1.1 General Methods

Unless stated otherwise, all reagents and solvents were purchased from Aldrich Chemicals and used without further purification. The syntheses of the hybrid organic-inorganic rotaxanes were carried out in Erlenmeyer Teflon® FEP flasks supplied by Fisher. Dry tetrahydrofuran was obtained by passing the solvent (HPLC grade) through an activated alumina column on a PureSolvTM solvent purification system (InnovativeTechnologies Inc., MA). Dry 1,4-dioxane was purchased from Acros Organics. Column chromatography was carried out using Silica 60 A (particle size 35-70 μm, Fisher, UK) as the stationary phase, and TLC was performed on pre-coated silica gel plates (0.25 mm thick, 60 F_{254}, Merck, Germany). NMR spectra were recorded on Bruker AV 300 and Bruker AV400 instruments. Chemical shifts are reported in parts per million (ppm) from low to high frequency and referenced to the residual solvent resonance. ESI mass spectrometry and elemental analyses were performed by departmental services at The University of Manchester. Carbon, nitrogen and hydrogen analysis was performed using a Flash 200 elemental analyser. Metal analysis was performed by Thermo iCap 6300 Inductively Coupled Plasma Optical Emission Spectroscopy (ICP-OES).

Magnetic Measurements. Variable-temperature (2.0–300 K) direct current (dc) magnetic susceptibility measurements under an applied field of 1000 G and variable-field (0–7.0 T) magnetization measurements at low temperatures (2.0 and 4 K) were carried out for **3** constrained in eicosane with a Quantum Design MPMS-XL7 SQUID magnetometer. The susceptibility data were corrected for the diamagnetism of the constituent atoms, the eicosane and the sample holder.

Electron Paramagnetic Resonace Spectroscopy. Continuous wave X-band (*ca.* 9.5 GHz) EPR spectra of microcrystalline samples of **3** was recorded with a Bruker EMX580 spectrometer at the EPRSC National UK EPR Facility and Service at The University of Manchester. The data was collected at 5K using liquid helium. Spectral simulations were performed using the *EasySpin 4.5.5* simulation software.[S1]

1.2 Single Crystal X-ray Diffraction

Data Collection. X-ray data was collected at a temperature of 100 K on a Bruker X8 Prospector diffractometer with CuK_α radiation, (λ = 1.54184Å) for compound **1**, equipped with an Oxford Cryosystems Cobra nitrogen flow gas system. Data was measured using Apex 2 suite of programs. X-Ray data for compound **3** was collected at a temperature of 240 K using a synchrotron radiation at single crystal X-ray diffraction beamline I19 in Diamond light Source,[S2] equipped with Saturn 724+ CCD detector and an Oxford Cryosystems Cobra nitrogen flow gas system. Data was measured using CrystalClear-SM Expert 2.0 r5 suite of programs.

Crystal structure determinations and refinements. X-Ray data was processed and reduced using CrysAlisPro suite of programmes. Absorption correction was performed using empirical methods (SCALE3 ABSPACK) based upon symmetry-equivalent reflections combined with measurements at different azimuthal angles.[S3] In compound **1**, all the atoms were refined anisotropically. Hydrogen atoms were placed in calculated positions, refined using idealized geometries (riding model) and assigned fixed isotropic displacement parameters. Disorder of the pivalate ligand was modelled over two positions. C-C distances were restrained to be equal using SADI command. Atomic displacement parameters were also restrained using RIGU.

Despite the use of an intense X-ray source (Diamond Light Source synchrotron), crystals of **3** diffracted only to 1.4 Å. Crystals of **3** were also found to be

commensurately modulated, presenting a q vector (½, 0, ½) (Figure S1a). Several attempts of solving this complicate crystallographic problem were done using JANA 2006 software, but due to the extreme complexity of the molecule and the lack of resolution, a proper solution wasn't obtained.

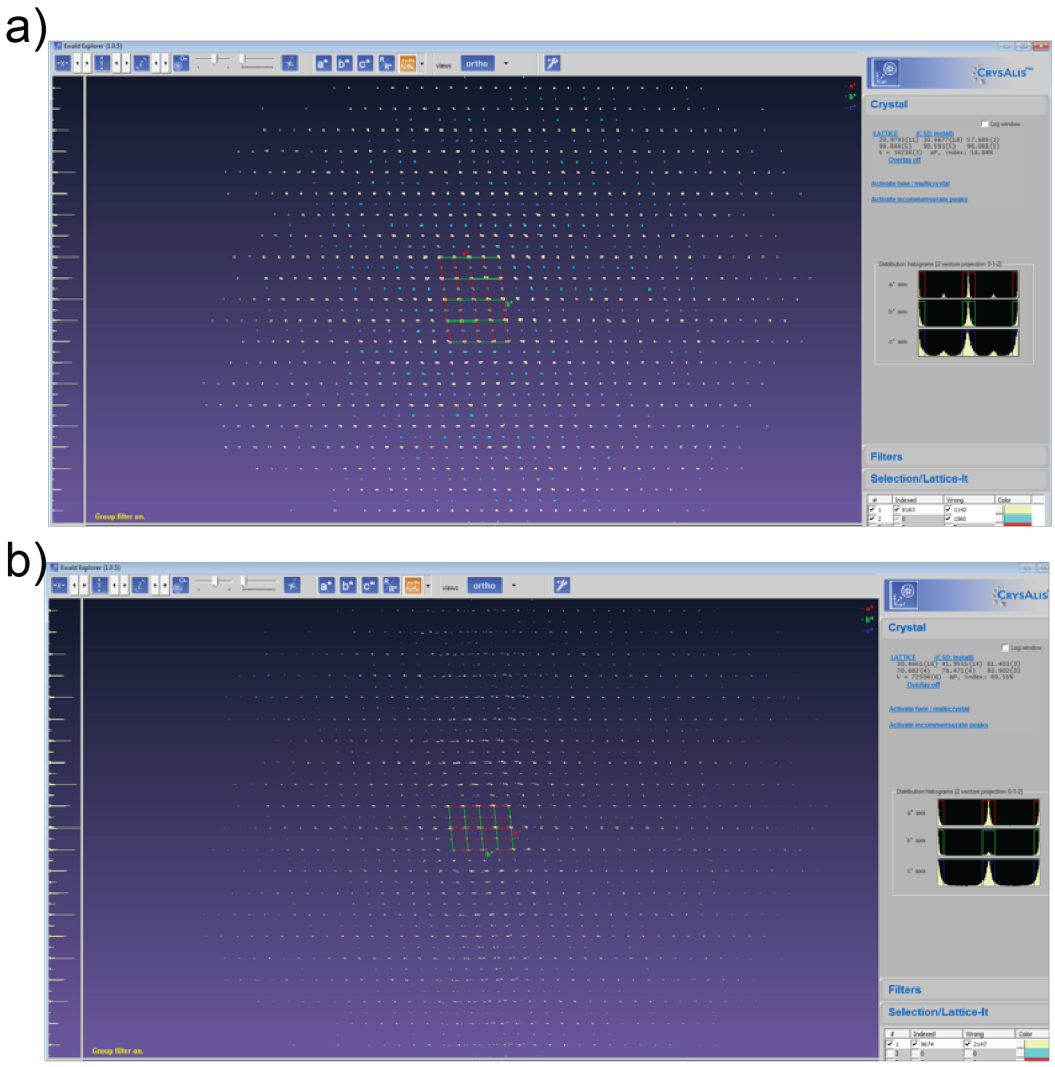

Fig S1. Ewald reciprocal space plot showing a) the subcell in white reflexions and the commensurate satellite reflexions in blue. b) The supercell where the subcell and the commensurate satellite reflexions are included.

In order to obtain an accurate model of the crystal structure, the supercell was chosen (Figure S1b). The crystal structure was solved and refined against all F^2 values using the SHELXL and Olex 2 suite of programmes.[S4] All atoms were refined isotropically with the exception of some Cr, Ni, Co and Fe metal atoms. Hydrogen atoms were omitted in the model but included in the formula. Due to the commensurately modulation found, two Cr_7Ni metallocrown and the corresponding threads were disordered. Despite several attempts of modelling the disorder in both rotaxanes, only one disordered metallocrown model was obtained (Figure S2).

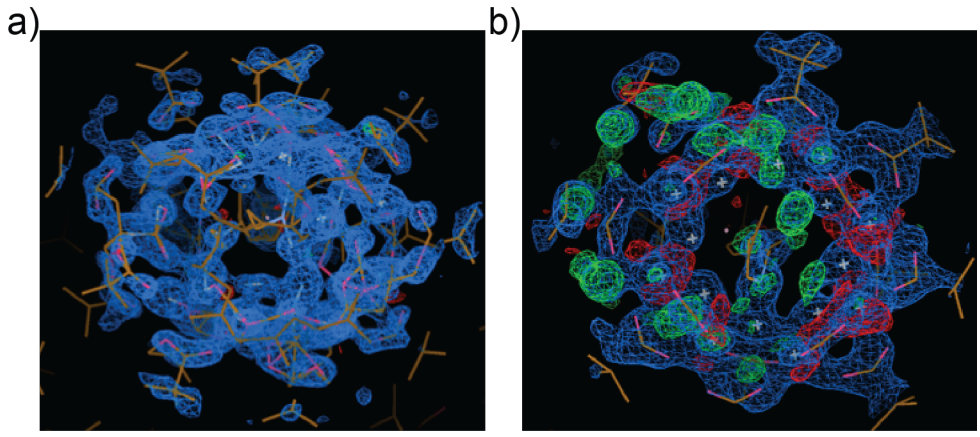

Fig S2. 2Fo-Fc electron density maps showing a) the modelled disorder and b) the unmodelled disordered of in a Cr_7Ni metallocrown. Chromium and nickel atoms in white, oxygen in pink, nitrogen in blue and carbon in orange. Electron density map in blue and remaining positive electron density map in red and negative in green.

In order to model the disorder in the structure, DFIX, SADI and SAME commands were used to restrain the geometry of pivalates, Cr-F-Cr and the thread. A large number of A alerts were found due to the crystal poor resolution (1.4 Å). Unfortunately this resolution is common in big molecules with big intermolecular spaces filled with disordered solvent molecules. This effect is also common in proteins, so a similar approach (Rigid Body) was used to solve the structure of the **3** coordination polymer.

As we can observe in Figure S3, the structural model was built on a broad shaped electron density map due to the poor resolution 1.4 Å of the data collected. Pivalate ligands were especially poorly resolved due to the most probable disorder of the group. As consequence the values of R1, wR and wR2 factors are larger than for standard crystal structures.

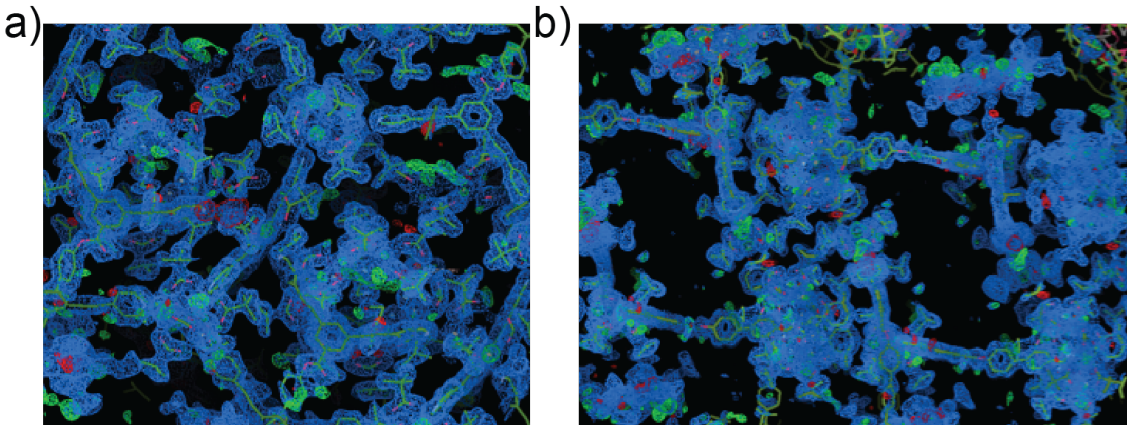

Fig S3. 2Fo-Fc electrondensity maps showing a) the (100) and b) (010) direction packing. Colour code as Figure S2.

Solvent mask protocol in Olex 2 was implemented to account with the remaining electron density corresponding to disordered molecules of tetrahydrofuran. A total of 2102 electrons were found un-accounted in the model. So 1051 electrons per formula unit were unaccounted, which may correspond to 28 THF solvent molecules.

CCDC 1572780 and 1572781 contains the supplementary crystallographic data for this paper. These data can be obtained free of charge *via* www.ccdc.cam.ac.uk/conts/retrieving.html (or from the Cambridge Crystallographic

Data Centre, 12 Union Road, Cambridge CB21EZ, UK; fax: (+44)1223-336-033; or deposit@ccdc.cam.ac.uk).

1.3 Synthesis

1.3.1 Synthesis of organic thread

(4'-phenethylamino)methyl-1,1'-biphenyl-4-ol (A):

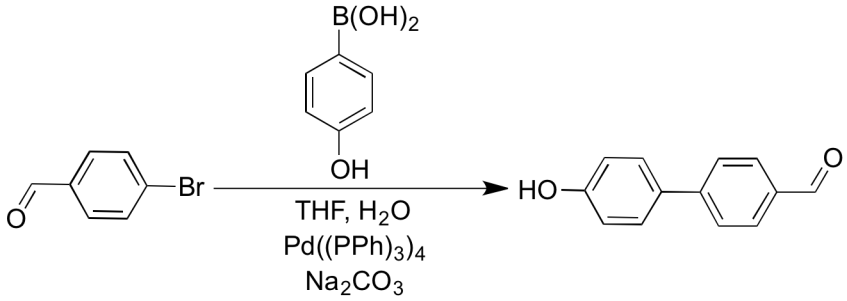

Fig S4. Schematic representation of the Suzuki-Miyaura cross-coupling reaction of 4-bromobenzaldehyde with 4-hydroxybenzeneboronic acid.

4'-hydroxy-[1,1'-biphenyl]-4-carbaldehyde: To a solution of 4-bromobenzaldehyde (1.3 g, 7.03 mmol) in 60 mL of THF and 30 mL of H_2O, 4-hydroxybenzeneboronic acid (1 g, 7.25 mmol) and Na_2CO_3 (3.5 g) were added and the solution was purged with N_2 for 15 min. $Pd(PPh_3)_4$ (10 % molar) was added to the flask and the mixture heated at 80 °C for 18 hours under nitrogen atmosphere. The reaction mixture was then poured into water, extracted with ethyl acetate (2 x 50 mL) and dried with anhydrous magnesium sulphate and evaporated. The crude reaction mixture was purified by recrystallization from hot toluene to give 4'-hydroxy-[1,1'-biphenyl]-4-carbaldehyde as a white solid in 56 % yield (0.8 g). ESI-MS (sample dissolved in MeOH, run in MeOH): m/z = 198 [M]. ^{1}H NMR (300 MHz, 293 K, $CDCl_3$,): δ = 4.98 (s, 1H); 6.94 (d, 2H); 7.55 (d, 2H); 7.71 (d, 2H); 7.93 (d, 2H); 10.04 (s, 1H). ^{13}C NMR (75 MHz, 293K, $CDCl_3$): δ = 116.5, 122.8, 129.71, 130.59, 131.13, 131.93, 143.26, 159.60, 187.31.

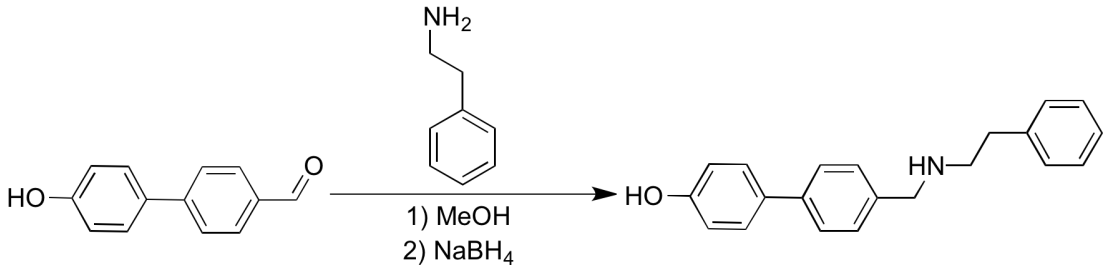

Fig S5. Schematic representation of the Schiff base condensation reaction of 4'-hydroxy-[1,1'-biphenyl]-4-carbaldehyde with phenylethylamine, followed by the reduction of the imine bond to generate a secondary amine.

(4'-phenethylamino)methyl-1,1'-biphenyl-4-ol: To a solution of 4'-hydroxy-[1,1'-biphenyl]-4-carbaldehyde (0.7 g, 3.6 mmol) in 30 mL of methanol, phenylethylamine (0.44 mL, 3.6 mmol) in 5 mL methanol was added and the reaction mixture was refluxed for 5 h under nitrogen atmosphere, allowed to stir at room temperature overnight. $NaBH_4$ (5 equivalents) was added and reaction mixture was stirred during 12 h under nitrogen atmosphere. The reaction was quenched with water and the solvent was evaporated. The solid was redissolved in chloroform (60 mL),

washed with water (2x 50 mL) and dried over anhydrous magnesium sulphate and evaporated. A white solid was obtained in 80 % yield (0.87 g). ESI-MS (sample dissolved in MeOH, run in MeOH): m/z = 304 $[M + H]^+$. ^{1}H-NMR (400 MHz, 293K, $CDCl_3$): δ = 2.81-2.93 (*m*, 4H); 3.90 (*s*, 2H); 6.8 (*d*, 2H, *J* = 7.9 Hz); 7.1-7.3 (*m*, 6H); 7.5-7.7 (*m*, 5H). ^{13}C NMR (75 MHz, 293K, $CDCl_3$): δ = 50.2; 53.7; 111.6; 123.6; 125.1; 125.6; 126.1; 126.8; 135.2; 137.4; 139.2; 140.5; 141.6; 142.8; 157.4.

1.3.2 Synthesis of organic ligand

3,5-bis(pyridin-4-ylethynyl)benzoic acid:

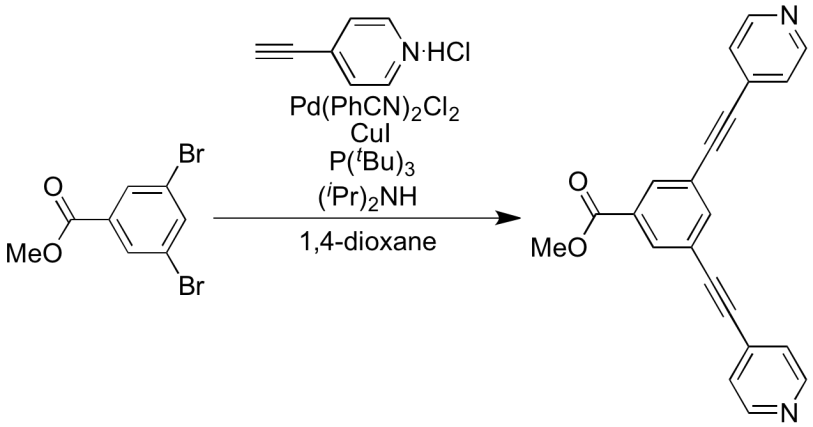

Fig S6. Schematic representation of the Sonogashira reaction of methyl 3,5-dibromobenzoate with 4-ethynylpiridine hydrochloride.

3,5-bis(pyridin-4-ylethynyl)benzoate: A mixture of methyl 3,5-dibromobenzoate (0.43 g, 1.4 mmol), 4-ethynylpiridine hydrochloride (0.39 g, 2.8 mmol), copper(I) iodide (11.4 mg, 0.06 mmol) and bis(benzonitrile)palladium(II) dichloride (34 mg, 0.09 mmol) were added to a 50 mL round bottom flask. After several cycles of pumped under vacuum and refilled with argon, degassed anhydrous 1,4-dioxane (30 mL), diisopropylamine (1.3 mL, 2.6 mmol) and tri(*t*butyl)phosphine (10 % solution in hexane, 0.35 mL, 0.14 mmol) were added through a canula and the dark brown suspension was stirred at 50 ºC for 20 hours. After cooling to room temperature, dichloromethane (25 mL) was added and the reaction mixture was filtered and the solvent removed under reduced pressure. The resulting residue was purified by column chromatography. First dichloromethane, followed by 40:1 dichloromethane:ethyl acetate was used, which allowed unreacted methyl 3,5-dibromobenzoate to be eluted. Thereafter increasing ratios of ethyl acetate were used eluting methyl 3,5-bis(pyridin-4-ylethynyl)benzoate. The solvent was removed under reduced pressure and a white solid was obtained in 80 % yield (0.4 g). ESI-MS sample dissolved in MeOH, run in MeOH): m/z = 338 $[M + H]^+$. ^{1}H-NMR (400 MHz, 293K, $CDCl_3$): δ = 3.81 (*s*, 3H); 7.3 (*d*, 4H); 7.8 (*s*, 1H); 8.2 (*s*, 2H); 8.7 (*d*, 4H). ^{13}C NMR (75 MHz, 293K, $CDCl_3$): δ = 50.1; 84.2; 87.7; 124.1; 125.6; 129.5; 132.5; 137.0; 150.5; 171.4.

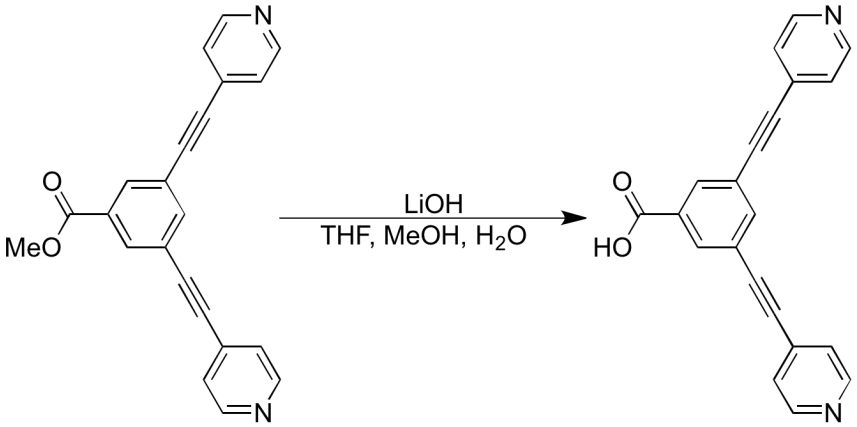

Fig S7. Schematic representation of the hydrolysis reaction of 3,5-bis(pyridin-4-ylethynyl)benzoate.

3,5-bis(pyridin-4-ylethynyl)benzoic acid: A mixture of 3,5-bis(pyridin-4-ylethynyl)benzoate (0.6 g, 1.7 mmol), lithium hydroxide (0.09 g, 0.5 mmol) in THF/MeOH/H_2O (30/20/6 mL) was stirred for 24 h at room temperature under nitrogen atmosphere. Then the THF and MeOH were removed under reduced pressure. The remaining water solution was acidified to pH 5 giving a white precipitate, which was collected by filtration, washed with water, and dried under vacuum to give 3,5-bis(pyridin-4-ylethynyl)benzoic acid in 81 % yield (0.5 g). ESI-MS sample dissolved in MeOH, run in MeOH): m/z = 325 $[M + H]^+$. ^{1}H-NMR (400 MHz, 293K, d_8-THF/*d*-TFA): δ = 7.7 (*d*, 4H); 7.8 (*s*, 1H); 8.4 (*s*, 2H); 9.2 (*d*, 4H). ^{13}C NMR (75 MHz, 293K, d_8-THF/*d*-TFA): δ = 89.4; 90.4; 124.8; 125.0; 131.9; 132.8; 134.1; 171.4.

1.3.3 Synthesis of [2]-rotaxanes

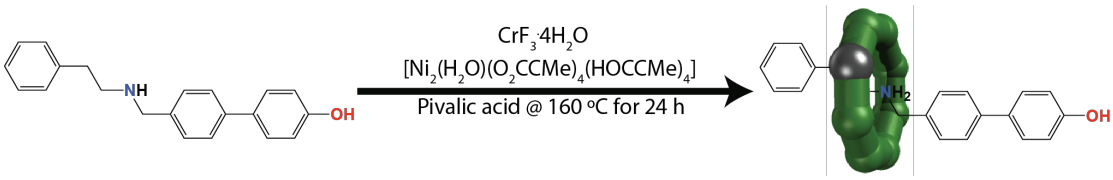

Fig S8. Schematic representation of the synthesis of hybrid organic-inorganic [2]-rotaxane **1**.

[HA{$Cr_7Ni(\mu$-F)$_8(O_2C^tBu)_{16}$}] (1): Pivalic acid (20.0 g, 195 mmol), (4'-phenethylamino)methyl-1,1'-biphenyl-4-ol (0.5 g, 1.7 mmol), and $CrF_3 \cdot 4H_2O$ (2.1 g, 12 mmol) were heated at 140 ºC with stirring in a Teflon flask for 0.5 h, then $[Ni_2(H_2O)(O_2CCMe_2)_4(HO_2CCMe_2)_4]$ (1.2 g, 2.5 mmol) was added. After 1 h the temperature of the reaction was increased to 160 ºC for 24 h. The flask was cooled to room temperature, and then acetonitrile (35 mL) was added while stirring. The green microcrystalline product was collected by filtration, washed with a large quantity of acetonitrile (200 mL), dried in air, washed with acetone and toluene, and then the remaining solid was extracted with THF to afford the desired product **1** as a green crystalline solid (1.5 g) in 35 % yield. X-ray quality crystals were obtained for **1** by recrystallization from THF/MeCN. ESI-MS (sample dissolved in THF, run in MeOH): m/z = 2474 $[M + H]^+$; 2497 $[M + Na]^+$. Elemental analysis (% calcd., % found for $C_{101}H_{166}Cr_7F_8NNiO_{33}$): C (48.58, 48.98), H (6.70, 6.71), Cr (14.58, 14.71), N (0.56, 0.49), Ni (2.35, 2.02).

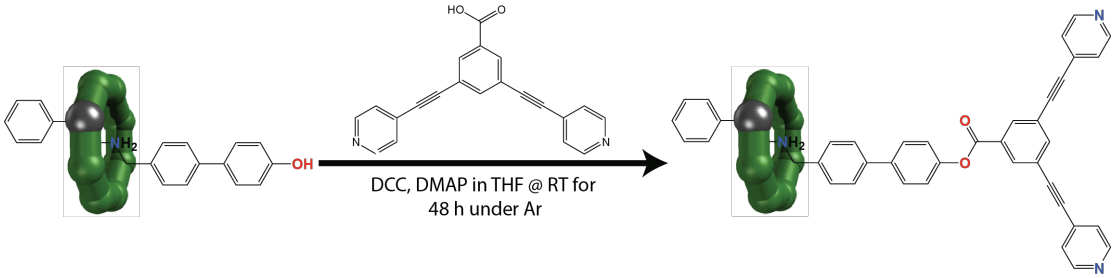

Fig S9. Schematic representation of the Steglich esterification reaction of 3,5-bis(pyridin-4-ylethynyl)benzoic acid with **1**.

[HB{Cr$_7$Ni(μ-F)$_8$(O$_2$C^{t}Bu)$_{16}$}] (2): A mixture of **1** (1.20 g, 0.5 mmol), 3,5-bis(pyridin-4-ylethynyl)benzoic acid (0.16 g, 0.5 mmol), dicyclohexylcarbodiimide (0.10 g, 0.5 mmol) and 4-(dimethylamino)pyridine (0.06 g, 0.5 mmol) in THF (10 mL) was stirred for two days at room temperature under an argon atmosphere. The reaction mixture was filtered to remove the dicyclohexylurea formed and the solvent evaporated under reduced pressure. The resulting residue was purified by column chromatography. First toluene, followed by 60:1 toluene:ethyl acetate was used, which allowed **1** to be eluted, leaving the products of the reaction at the top of the column. Thereafter 10:1 toluene:ethyl acetate was used, eluting **2**. The solvent was removed under reduced pressure. Crystals of **2** were obtained from recrystallization from THF/MeCN, but they do not diffract well enough to give a high-resolution structure (0.48 g, 40 %). ESI-MS (sample dissolved in THF, run in MeOH): (*m*/*z*) = 2804 $[M + H]^+$; 2826 $[M + Na]^+$. Elemental analysis (% calcd., % found for $C_{122}H_{178}Cr_7F_8N_3NiO_{34}$): C (52.26, 52.51), H (6.36, 6.39), Cr (12.98, 13.32), N (1.50, 1.66), Ni (2.09, 2.01).

1.3.4 Synthesis of polymeric [c2]-daisy chain

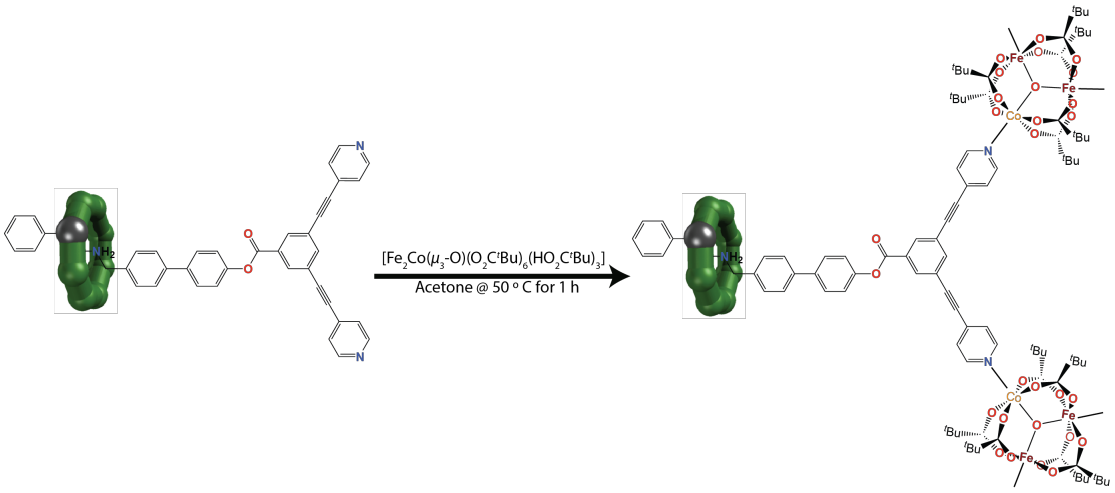

Fig S10. Schematic representation of the synthesis of polymeric [c2]-daisy chain **3**.

[[HB{Cr$_7$Ni(μ-F)$_8$(O$_2$C^{t}Bu)$_{16}$}]$_3$[Fe$_2$Co(μ_3-O)(O$_2$C^{t}Bu)$_6$(HO$_2$C^{t}Bu)$_3$]$_2$] (3): Compound **2** (84.15 mg, 0.03 mmol) was dissolved in hot acetone (5 mL). A solution of [Fe$_2$Co(μ_3-O)(O$_2$C^{t}Bu)$_6$(HO$_2$C^{t}Bu)$_3$] (21.99 mg, 0.02 mmol) in acetone (3 mL) was added dropwise and the green solution was stirred at 50 ºC for 1 hour. The solvent was removed under reduced pressure and X-ray quality crystals were obtained for **3** by recrystallization from THF/MeCN (3:1) (151.71 mg, 75 % isolated yield). Elemental analysis (% calcd., % found for $C_{426}H_{642}Co_2Cr_{21}F_{24}Fe_4N_9Ni_3O_{128}$): C (51.15, 50.19), H (6.47, 6.02), Cr (10.92, 10.73), N (1.26, 1.20), Ni (1.76, 1.80), Fe (2.23, 3.23), Co (1.18, 1.20).

[[HB{$Cr_7Co(\mu\text{-}F)_8(O_2C^tBu)_{16}$}]$_3$[$Fe_2Co(\mu_3\text{-}O)(O_2C^tBu)_6(HO_2C^tBu)_3$]$_2$] ($\mathbf{3^{Co}}$):

The analogous compound but featuring a {Cr_7Co} ring can be made by an analogous route, but using [$Co_2(H_2O)(O_2CCMe_2)_4(HO_2CCMe_2)_4$] in the step to make $\mathbf{1^{Co}}$.

Elemental analysis (% calcd., % found for $C_{426}H_{642}Co_5Cr_{21}F_{24}Fe_4N_9O_{128}$): C (51.14, 50.59), H (6.47, 6.39), Cr (10.92, 10.49), N (1.26, 1.25), Fe (2.23, 3.31), Co (2.95, 2.99).

Thermogravimetric analysis of $\mathbf{3^{Co}}$ shows decomposition of the sample at around 350 ° C (see below).

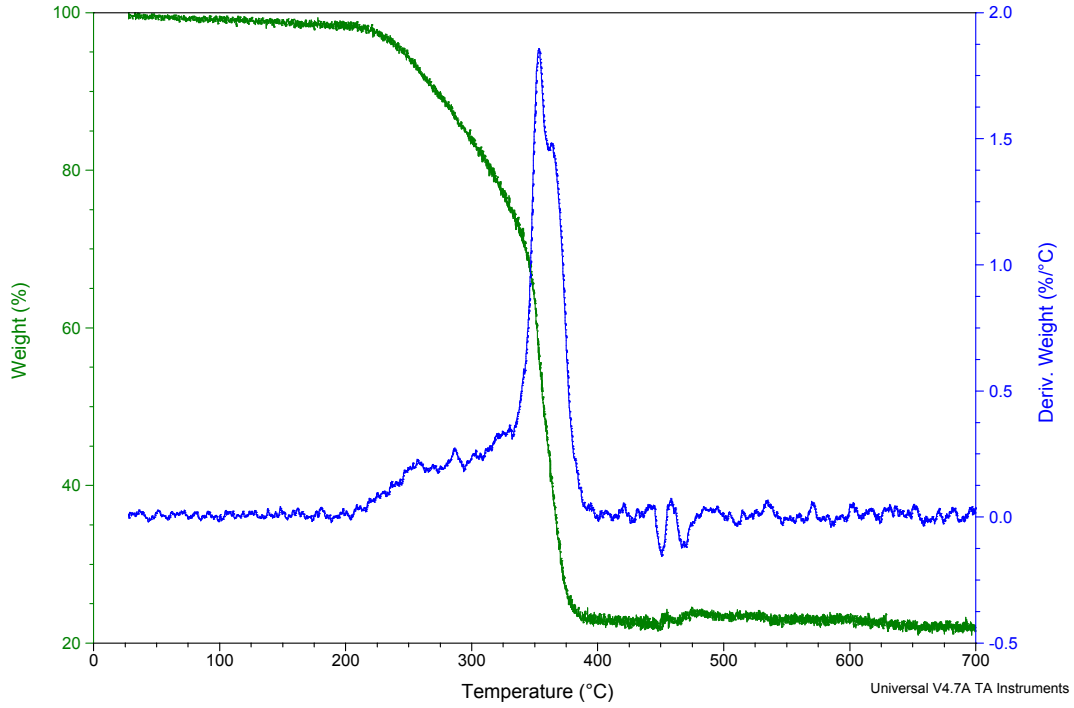

2. Supplementary Figures

2.1 Crystal Structures

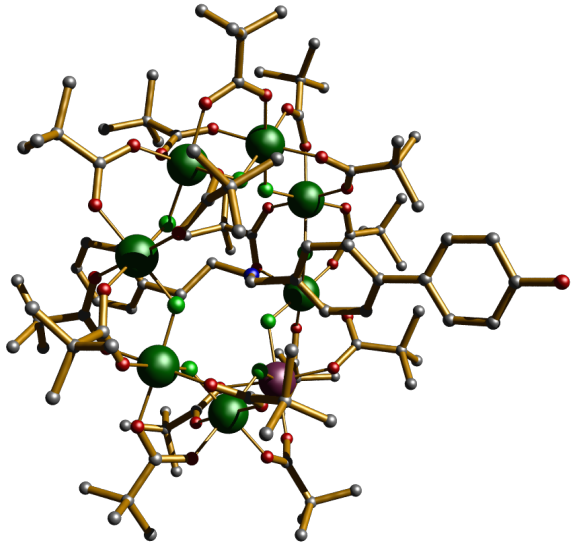

Fig S11. X-ray single crystal structures of **1**. Colour code: Cr, green; Ni, purple; N, blue; O, red; C, grey; F, pale green. H atoms omitted for clarity.

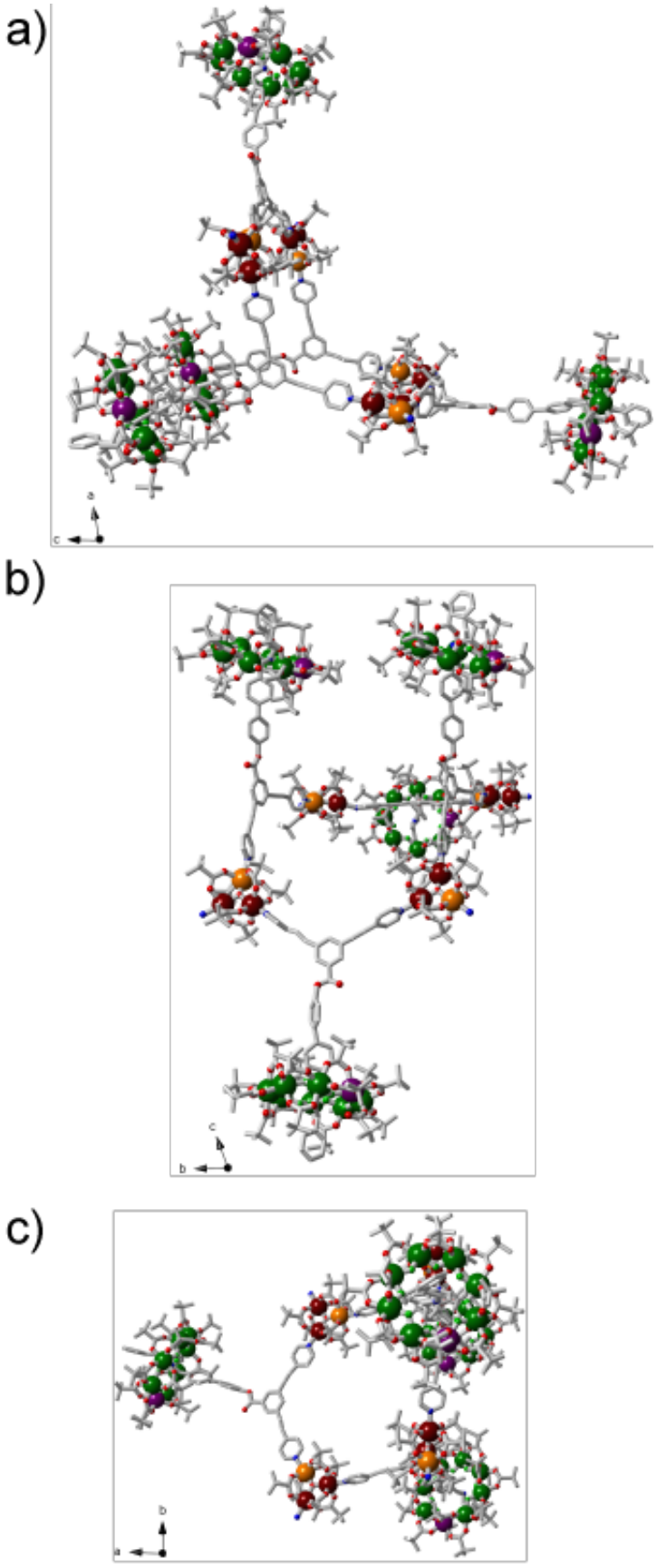

Fig S12. Perspective views of a fragment of one single interlocked ladder in **3** along the crystallographic *b* (a), *a* (b) and *c* (c) axis. Colour code: Co, orange; Cr, green; Ni, purple; Fe, brown; N, blue; O, red; C, grey; F, pale green.

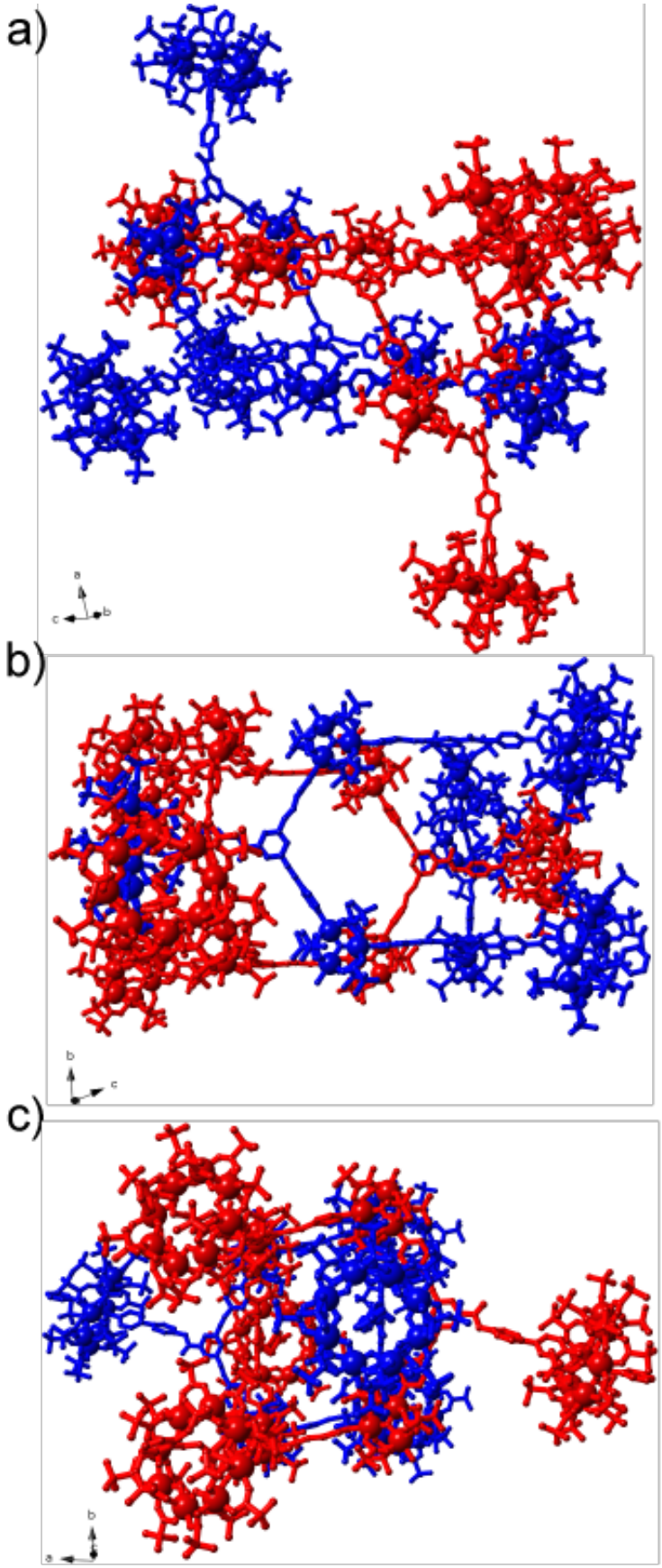

Fig S13. Perspective views of a fragment of two doubly interlocked ladders in **3** along the direction 111 (a) and the crystallographic *bc* (b) and *ba* (c) planes.

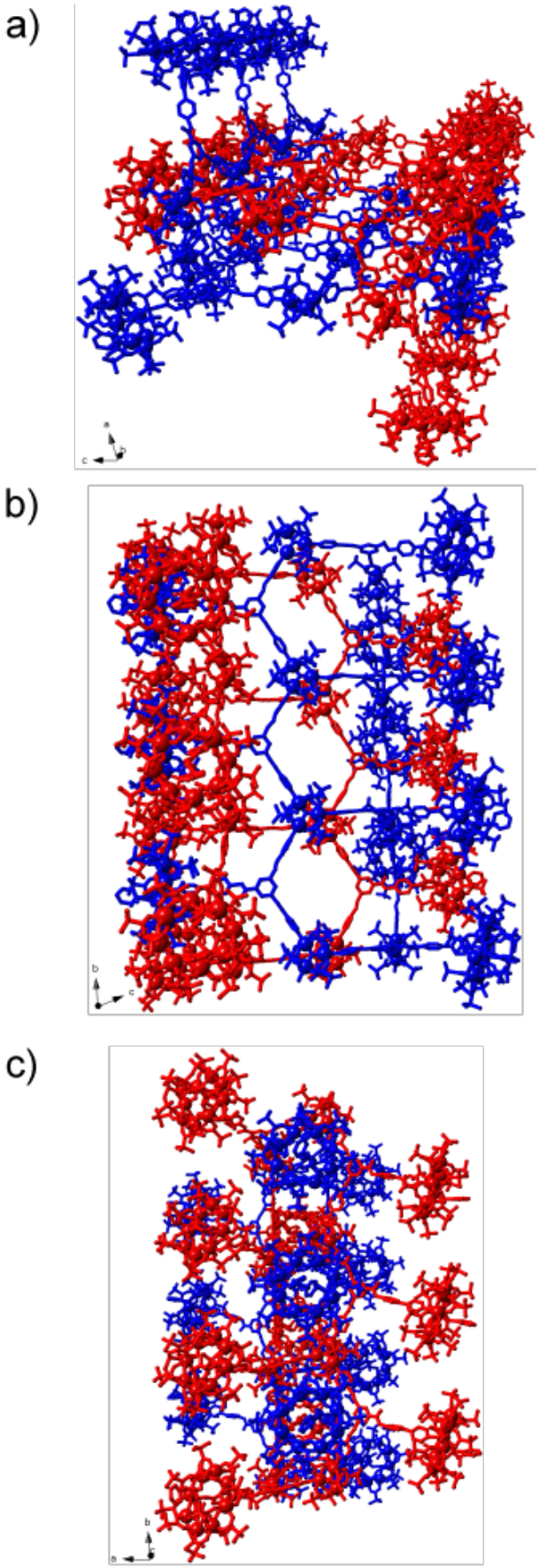

Fig S14. Perspective views of the polymeric interlocked [c2]-daisy chain in **3** along the direction 111 (a) and the crystallographic *bc* (b) and *ab* (c) planes.

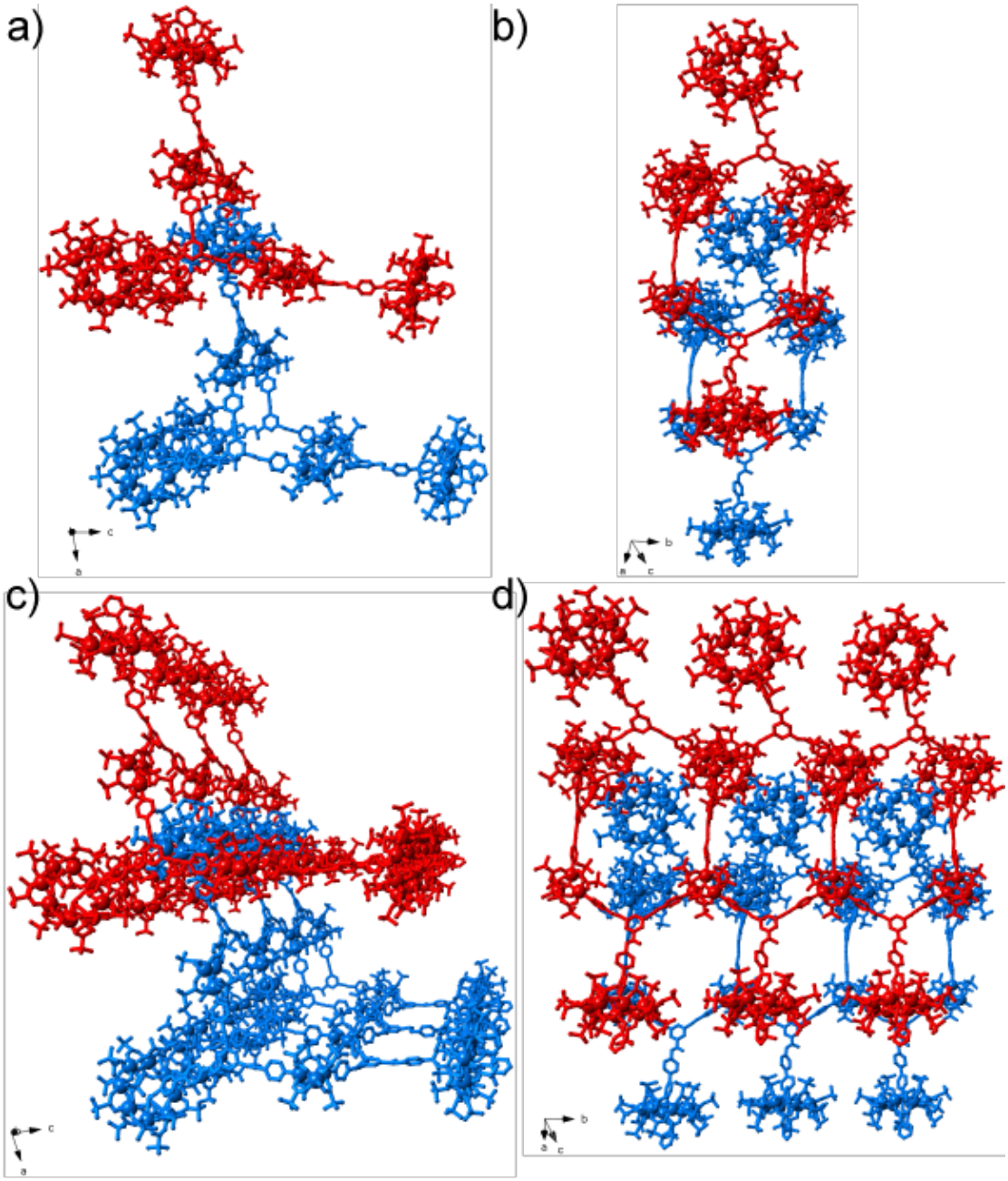

Fig S15. Perspective view of a fragment of two neighboring interpenetrated single interlocked ladders in **3**.

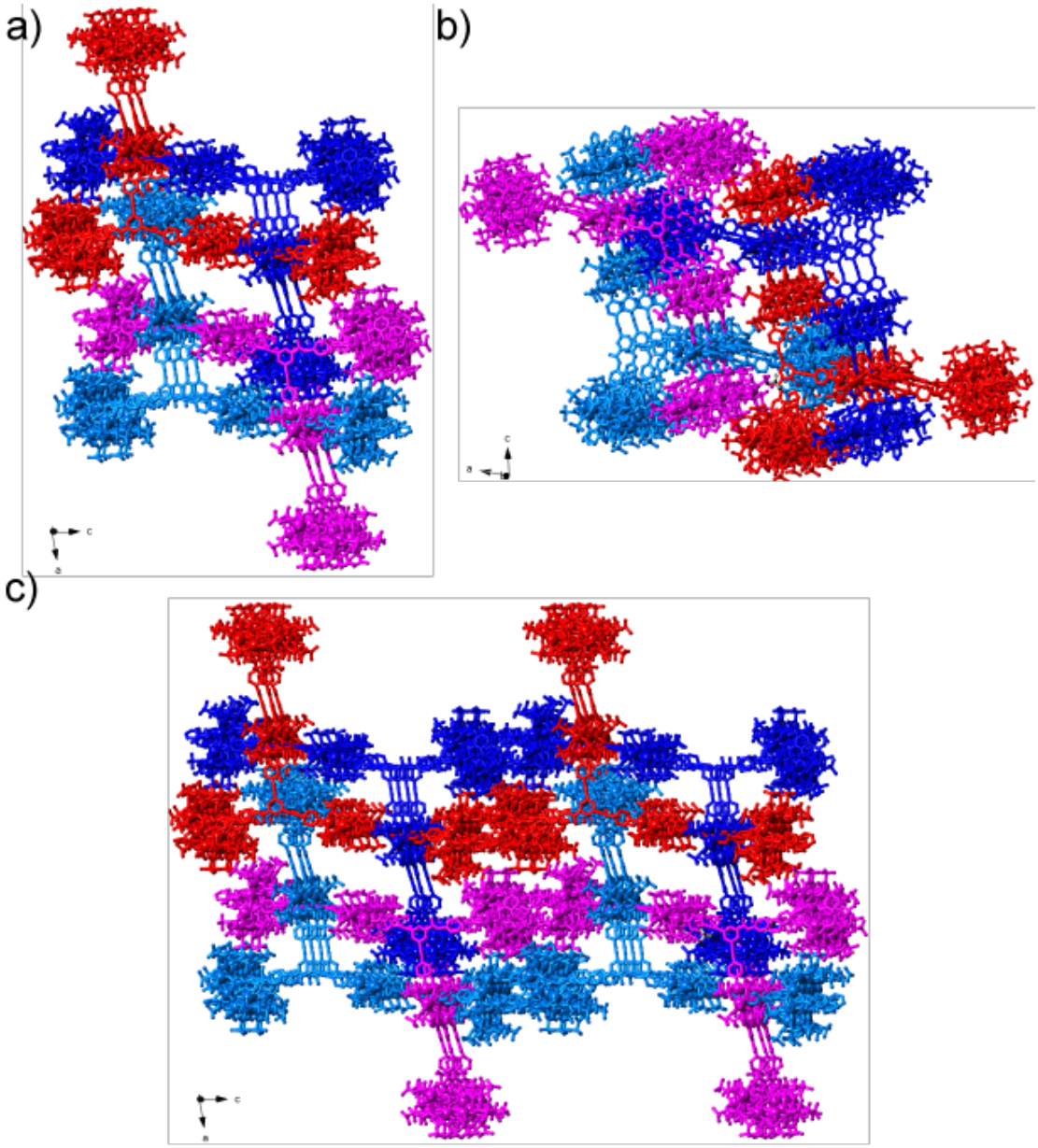

Fig S16. Crystal packing of **3** showing the interpenetration between neighboring polymeric [c2]-daisy chains. The adjacent polymeric daisy chains are colored in pale blue-pink and in deep blue-red, respectively.

2.2 Magnetic Measurements

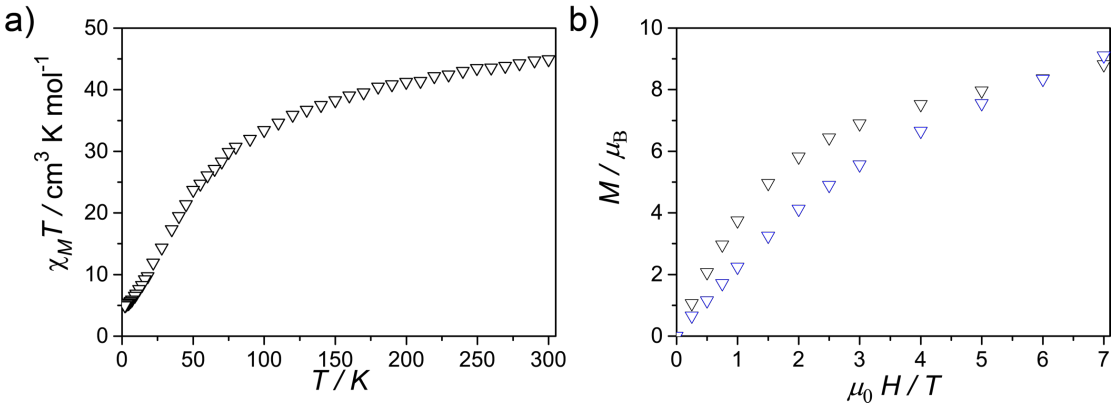

Figure S17. Temperature dependence of the product of the direct current (dc) molar magnetic susceptibility by the temperature ($\chi_M T$) (a) and the magnetic field dependence of the molar magnetisation (M) at 2 (▽) and 4 (▽) K (b) for **3**.

2.3 Electron paramagnetic resonance spectroscopy

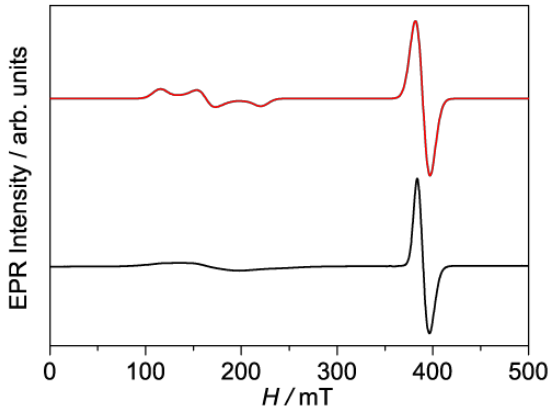

Figure S18. Experimental (black trace) and simulated (red trace) X-band continuous wave electron paramagnetic resonance on powder of **3** at 5K.

3. Supplementary Tables

Table S1. Crystallographic information for compounds **1** and **3**.

	1	**3**
Crystal colour	Green	Green
Crystal size (mm)	0.30 × 0.20 × 0.10	0.40 × 0.10 × 0.10
Crystal system	Orthorhombic	Triclinic
Space group, *Z*	Pbcn, *8*	P-1, *2*
a (Å)	28.7006(4)	30.4435(10)
b(Å)	30.9417(6)	41.9494(12)
c (Å)	33.8959(6)	61.4185(19)
α (°)	90	70.698(3)
β (°)	90	78.434(3)
γ (°)	90	83.927(3)
V (Å^3)	30101.1(9)	72458(4)
Density (Mg.m^{-3})	1.276	0.916
Wavelength (Å)	1.54184	0.6889
Temperature (K)	100	240
μ(Mo-Kα) (mm^{-1})	4.827	0.530
2Θ range (°)	4.944 to 148.732	3.038 to 28.486
Reflns collected	222103	85717
Independent reflns (R_{int})	30035 (0. 1176)	54442 (0. 1204)
L.S. parameters, *p*	1690	5324
No. of restraints, *r*	286	203029
*R*1 (*F*)[a] *I* > 2.0σ*(I)*	0.0991	0.2248
*wR*2(*F*^{2}),[a] all data	0.2856	0.5684
S(*F*^{2}),[a] all data	1.061	1.530

[a] $R1(F) = \Sigma(|F_o| - |F_c|)/\Sigma|F_o|$; [b] $wR^2(F^2) = [\Sigma w(F_o^2 - F_c^2)^2/\Sigma wF_o^4]^{½}$; [c] $S(F^2) = [\Sigma w(F_o^2 - F_c^2)^2/(n + r - p)]^{½}$

4. References of Supporting Information

S1. Stoll, S.; Schweiger, A. *J. Magn. Reson.* **2006**, *178*, 42.

S2. Nowell H, Barnett SA, Christensen KE, Teat SJ, Allan DR. J *Synchrotron Radiat*.,**2012**, *19*, 435-441.

S3. (a) G. M. Sheldrick, SADABS, empirical absorption correction program based upon the method of Blessing. (b) L. Krause, R. Herbst-Irmer, G. M. Sheldrick, D. Stalke, *J. Appl. Cryst*. **2015**, 48. (c) R. H. lessing, *Acta Crystallogr.* **1995**, *A51*, 33-38.

S4. a) Sheldrick. G. M., *Acta Crystallogr.*, **2015**, *C71*, 3-8; b) O. V. Dolomanov, L. J. Bourhis, R. J. Gildea, J. A. K. Howard, H. Puschmann,. *J. Appl. Cryst.*, **2009**, *42*, 339–341